Experimental investigation of sedimentation of a thin elastic membrane in a viscous fluid

Tymoteusz Miara,

School of Physics and Astronomy

The University of Manchester

Summer Work Laboratory Report

July 2016

Abstract

The bending of thin elastic PDMS membranes as they sediment or rise in a viscous fluid is investigated experimentally. The method of extracting a 3D shape of a membrane from a video recording is proposed. The final curvatures of bended strips of various aspect ratios are compared with an elastic slender rod theory. The width-dependence of the curvature is investigated. The metastable shapes are described. The sources of asymmetry in the membranes are discussed. Finally, the possible future applications in graphene industry are discussed.

1. Introduction

The physics behind sedimenting rigid bodies in a hyperviscous fluids is well understood [1-4]. A body falling in a viscous medium experiences gravitational force, buoyancy force and viscous resistance, which in case of laminar flow is proportional to velocity and is related to the shape of the body. The velocity at which those forces balance is called terminal velocity. It was shown that as body sediments, it will maintain its initial orientation and will drift horizontally at a certain angle depending on the inclination of its principal axes of rotation to the vertical (Happel & Brenner 1965). With flexible filaments the problem is much more complicated as the filament starts to change its shape and reorient. The sedimentation of flexible slender filaments was investigated numerically by Spagnolie *et al*. (2013) [5], where a dimensionless elasto-gravitational number was introduced to describe the final shape of the filament. In this work it will be of interest to experimentally investigate how the situation changes when instead of a filament, membranes (sheets) of different aspect ratios are considered. As the width of a membrane is small and approaches its thickness, the behaviour should be similar to that of a slender rod described in [5]. As the width becomes larger the body is no longer slender and its bending curvature might change. It is also interesting to investigate how the behaviour changes as membrane's thickness, which is related to bending stiffness, is varied.

2. Theoretical overview of the sedimentation of a slender elastic rod

Following [5], the dimensionless elasto-gravitational number for a slender rod is defined as:

$$\beta = \frac{\mathrm{EI}}{\mathrm{F_g\, L^2}}, \tag{1}$$

where E is Young's modulus of the body, I is the second moment of area, F_g is the net force of gravitational and buoyancy forces acting per unit length of the body and L is the length of the rod.

[5] considers the cases of a rods with circular cross-section and hence the second moment of area $I = \pi r^4/4$. However, in the case for a rod with rectangular cross-section, the second moment of area is $I = bh^3/12$, where b is the width of the rod and $h < b$ is its thickness. The area of this cross-section is $A = b\ h$. The net force of gravity and buoyancy per unit length is $F_g = A\ g\ \Delta\rho = b\ h\ g\ \Delta\rho$, where $\Delta\rho$ is the difference in densities of the body and of the fluid. It should be noted that if the body is rising in the fluid, the physics is no different than if it were falling. In the rising case it could be assumed that $\Delta\rho < 0$ and hence $\beta < 0$, but for convenience the absolute value will be used and the minus signs will be dropped.

According to [5], the number β alone is sufficient to describe the final shape of the filament. Hence, it is implied that viscosity scales out of the problem.

Substituting second moment of area and gravitational buoyancy forces into (1) we get:

$$\beta = \frac{\mathrm{E\ b\ h^3}}{12\ \mathrm{b\ h}\ \Delta\rho\ \mathrm{g\ L^2}} = \frac{E\ h^2}{12\ \Delta\rho\ \mathrm{g\ L^2}} \tag{2}$$

which is independent of the width b. This theory however is derived from a slender-body which assumes width being similar to height. As b>>h slight deviation can appear as the body is no longer slender. It is of interest of this work to establish this width dependence of β.

Another problem arises with predictions posed by [5] as only spheroidal filaments were considered and hence, due to the not uniform gravitational-buoyancy forces the curvature is much higher than if a uniform rod was considered.

3. Experimental Method

3.1 Set-up

The set-up consisted of a large beaker filled with ReAgent Glycerol Tech. The diameter of the beaker was 28 cm and the height of the fluid was 40 cm. The kinematic viscosity of the fluid at the temperature of 20 degrees of Celsius was measured by a suspended level shortened form viscometer to be 744 ± 4 cSt. Hence from tables [6] it can be established that it is 97% pure glycerol and hence it has density of (1256 ± 1) kg m^{-3}.

The membranes were made of thin PDMS film mostly of 0.1 mm thickness, but 0.05 mm sheets were also used. When cut with scissors, the sheets exhibited significantly asymmetric behaviour depending on which side was on top and which was on bottom. In order to minimise the plastic deformation introduced by cutting the material, a scalpel was used.

To measure Young's modulus of PDNMS sheets a simple experiment was conducted where a strip of known cross-sectional area was attached to a mass. Two points were marked on the strip and a video was taken to compare the distances between two points without any load and with load. Knowing the weight of the mass, cross-sectional area of the strip and relative elongation, Young's modulus was measured to be (620 ± 20) kPa.

The density of PDMS membranes was measured using an OHAUS scale to be (1208 ± 8) kg m^{-3}. Since it is lower than of glycerine, the sheets rise in the fluid. Placing them near bottom involved usage of a long spoon which bowl was bent perpendicularly to the handle. With this tool it is possible to suspend sheets in approximately flat initial position.

The deformation of the sheet as it rises was recorded either from the top (position 1) or from the side (position 2). The schematic of the set-up is shown of Figure 1.

Few hundreds of small dots were marked on the membranes in order to recover three-dimensional shape of the membranes using a single camera.

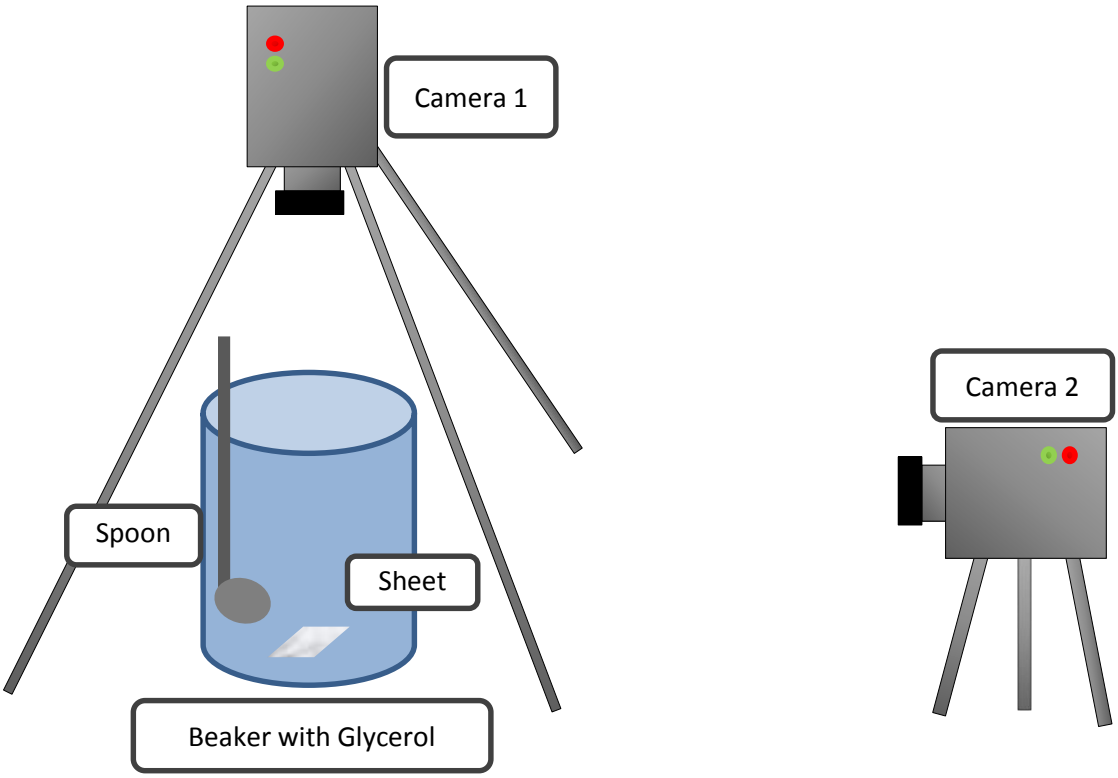

Figure 1 Schematic of the experimental setup. The camera was either in position 1 or 2.

3.2 Image analysis method.

3.2.1 The recovery of 3D shape of the membrane based on a recording from the camera in position 1.

Consider a flat, horizontal sheet with many dots on it recorded far away from above. As the sheet changes its shape, the dots appear to be moving relative to one another. The more the sheet becomes inclined in a certain place, the closer the points appear on the screen. Their relative distance as projected on the camera is changing. Hence, if the original (undeformed) pattern of the points is known, then it is possible to gain some information about the three dimensional shape as the membrane deforms.

Assuming the points are close to one another and the sheet does not stretch, the local curvature can be considered as small enough so that the spatial distance between nearest points remains the same. It therefore can be assumed that whatever change in distances is observed by the camera it is solely due to the inclination of the surface at that place. Hence, from Pythagorean theorem, if the spatial distance from point A to B is conserved and equals x, then if their projections on the screen A' and B' are x' apart, then $x^2 = x'^2 + h^2$, where h is the difference in the vertical position of points A and B.

There is however ambiguity: It is not possible to establish, whether point A is higher than point B by h, or vice versa. Hence, the rule determining which point (A or B) is higher and which is lower must be given *a priori* based on the independent observation. Fortunately, in most cases the membrane bends in a simple, symmetric, and partly monotonous shape, having a crest of the maximum height as shown on the Figure 2.

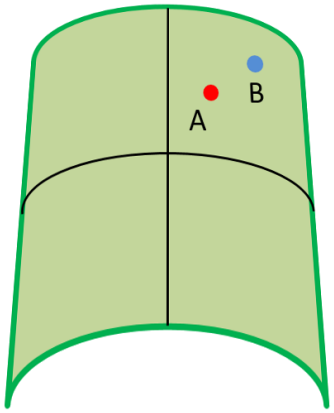

Figure 2 The qualitative shape of the membrane. Point A is assumed to be higher than B if it is closer to the line of local maxima.

The fact that the shape has the line of local maxima from which the heights are decreasing monotonically allows to set a rule that point A is higher than point B if A is closer to the line of local maxima (crest). The crest does not necessarily have to be in any of the axes of symmetry. It is possible for the membrane to tilt if the initial orientation was not perfectly horizontal. In that case, the position of the crest can be established by finding the points which form the lowest (approaching zero) inclination with their neighbours. This is easier done manually, by looking at the video, but can be done automatically.

The following algorithm was implemented in Mathematica 10.4 (see Appendix 1) to obtain the three dimensional shape of the sheet:

1. Track the positions of the dots and delete all incomplete tracks. Mathematica uses image cross-correlation for purpose of tracking.
2. Assume the first/last frame is the template of the position of the dots on undeformed surface. Find/get the point M that is in the middle of the crest.
3. Triangulate the points in the template frame using Delaunay Triangulation algorithm.
4. Based on the triangulation, construct a weighted adjacency matrix A with weights corresponding to the distances between adjacent points.
5. Using Dijkstra algorithm find the shortest paths from point M to every other point X.
6. For each next frame t, of the recording use a Pythagoras theorem to construct a weighted adjacency matrix B_t with weights representing the height difference between two adjacent points and use the described above rule to determine the sign.
7. For each frame t, find the height of every point X relative to the point M by summing the weights of matrix B_t (height differences) while going along the shortest path from M to X.
8. For each frame t, plot the three dimensional position of every point (the shape of the surface), assuming point M is at height 0.

To verify whether this algorithm works correctly, an experiment was conducted involving a sheet of paper marked with few hundred points 300 of which were tracked. The sheet was initially flat and then it was wrapped around a cylinder. The process was

recorded with a camera and the three dimensional image was obtained. Figure 3 shows the side-view of the points along with a fitted cylinder.

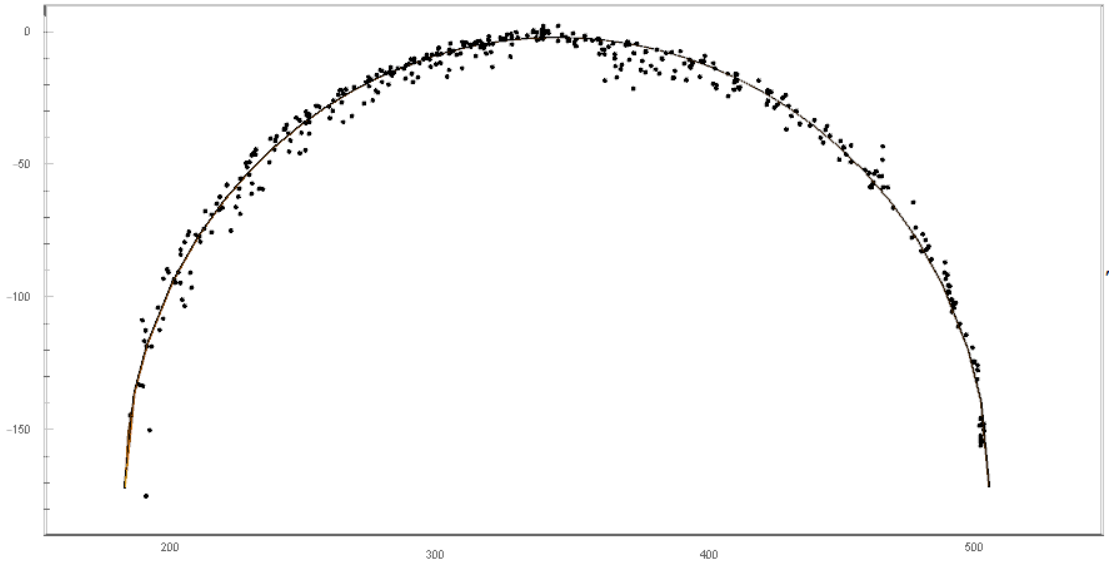

Figure 3 The side view of a recovered three-dimensional shape of a sheet wrapped around a cylinder. The best fit of a cylinder is plotted for comparison. This proves that the algorithm is working correctly with 2% accuracy.

There is a significant limitation to this method, however. If a membrane bends approaching the U shape or even more, some points become invisible to the camera and then the tracking algorithm loses them or switches to other (visible) points. If the former happens, the algorithm will delete them in the first step. If the latter happens, some of the edges connected with those disappearing points will be reduced largely, sometimes even to zero. It can also happen that some of the edges will become larger than initially resulting in the height difference being a complex number. If that happens to many inter-connected points, the result is non-physical, often resulting in some points being outliers, sometimes higher than 0. The situation when that happens is shown on Figure 4:

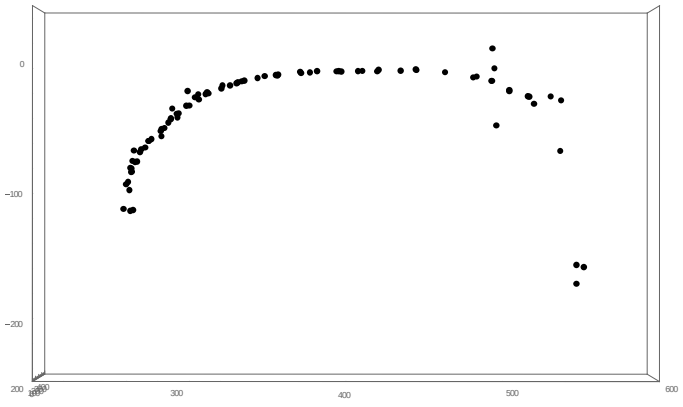

Figure 4 Side view of a strip. At the right-hand side some points are missing, and some are lying significantly out of place, even higher than zero. This happens when the sheet bends too much and the tracking algorithm switches dots.

Due to this inaccuracy, more accurate method of recording from the side should be used for purposes of measuring the curvature of membranes.

3.2.2 Recovery of the profile of the membrane when recorded from position 2.

Consider an object placed in the cylindrical beaker of radius R filled with fluid of refraction index n. Because of the translational symmetry in vertical direction, the system can be considered two-dimensional. Assume the origin of the co-ordinate system is in the centre of the beaker. Let the objects position be (x,y). This object (as observed from outside of the beaker) will appear to be in the position (x',y'). This position of the image can be calculated by considering the refraction of the rays shown on Figure 5.

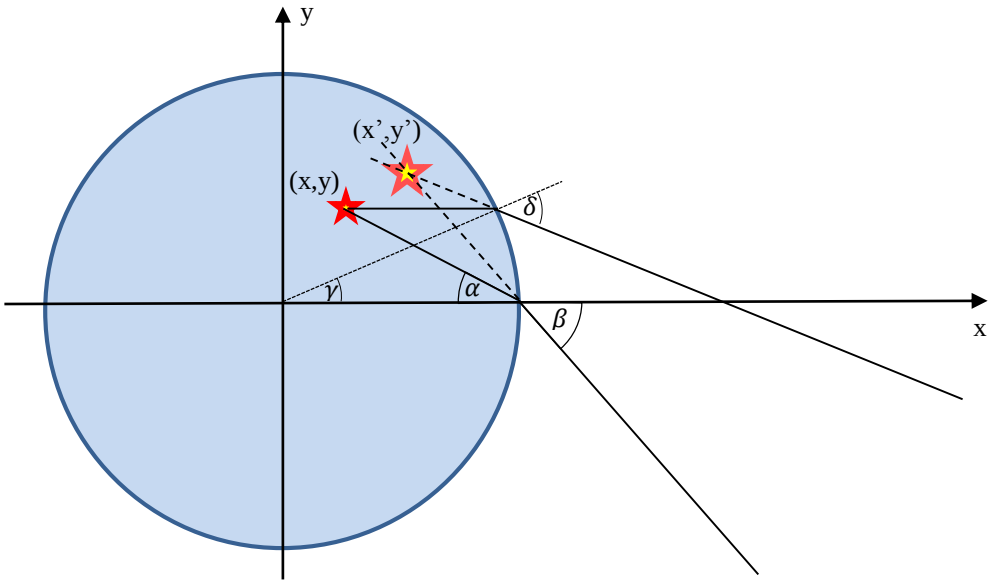

Figure 5. Top-view schematic showing the position of an object and its image in the beaker.

Applying Snell's law, the system is described by the following set of equations:

$$\tan\alpha = \frac{y}{R-x} \tag{3.1}$$

$$\sin\beta = n\sin\alpha \tag{3.2}$$

$$\sin\gamma = \frac{y}{R} \tag{3.3}$$

$$\sin\delta = n\sin\gamma \tag{3.4}$$

$$\tan\beta = \frac{y'}{R-x'} \tag{3.5}$$

$$\tan\delta - \gamma = \frac{y'-y}{R\cos\gamma - x'} \tag{3.6}$$

the solution of which is given by:

$$y'(x,y) = \frac{y\,n\left(R\left((x-R)\left(1-\sqrt{1-\frac{y^2}{R^2}}\right)\right)\tan\left(\sin^{-1}\left(\frac{y}{R}\right)-\sin^{-1}\left(\frac{yn}{R}\right)\right)+y(x-R)\right)}{(x-R)\left(yn-(x-R)\sqrt{\frac{y^2}{(x-R)^2}+1}\cdot\sqrt{1-\frac{y^2n^2}{y^2+x^2-2xR+R^2}}\cdot\tan\left(\sin^{-1}\left(\frac{y}{R}\right)-\sin^{-1}\left(\frac{yn}{R}\right)\right)\right)} \tag{4}$$

In case of narrow strips the most accurate way of measuring their curvature is by taking the picture from the side. The cylindrical beaker however, magnifies and distorts the

image. Applying equation (4) the image can be transformed to show the original shape of the object. This was done by inverting equation (4) to obtain y(y') relation and applying ImageForwardTransformation function in Mathematica 10.4.

To verify the accuracy of this correction, a paper with printed square lattice was dipped in the beaker and photographed from position 2. Then the image transformation was applied and the restored lattice was measured to be better than 2% accurate. The main source of error is the uncertainty in determining the x-position (offset from the origin) of the object. The photograph and a transformed image are shown on Figure 6.

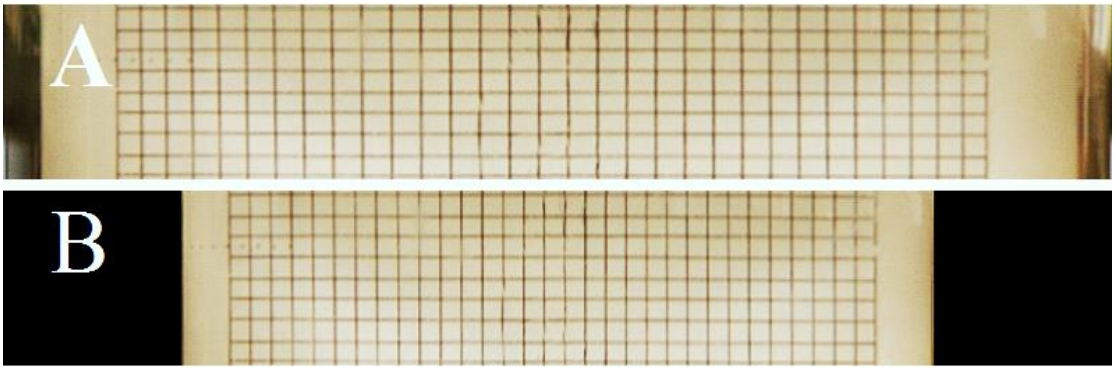

Figure 6 (A) The photograph of a square lattice printed on the paper dipped in beaker with glycerol. (B) The recovered image of the actual shape of the lattice.

Having the corrected image, circles were fitted to the pictures of membranes using video analysis software Tracker 4.92 and the curvature was obtained. Because of the boundary effects that could possibly cause asymmetry in the membranes, the curvature (the reciprocal of a radius of a cylinder tangent to the membrane) of the rising strips was measured separately in each orientation.

4. Experimental results and discussion

4.1 Thin strips

For strips of thickness 0.1 mm, length 80 mm, $\beta = (17 \pm 3) \cdot 10^{-5}$. The values of measured curvatures of strips ranging in width from 1mm to 30 mm are shown in Figure 7. Each point is based on four experiments and the error bars represent the standard error of the mean.

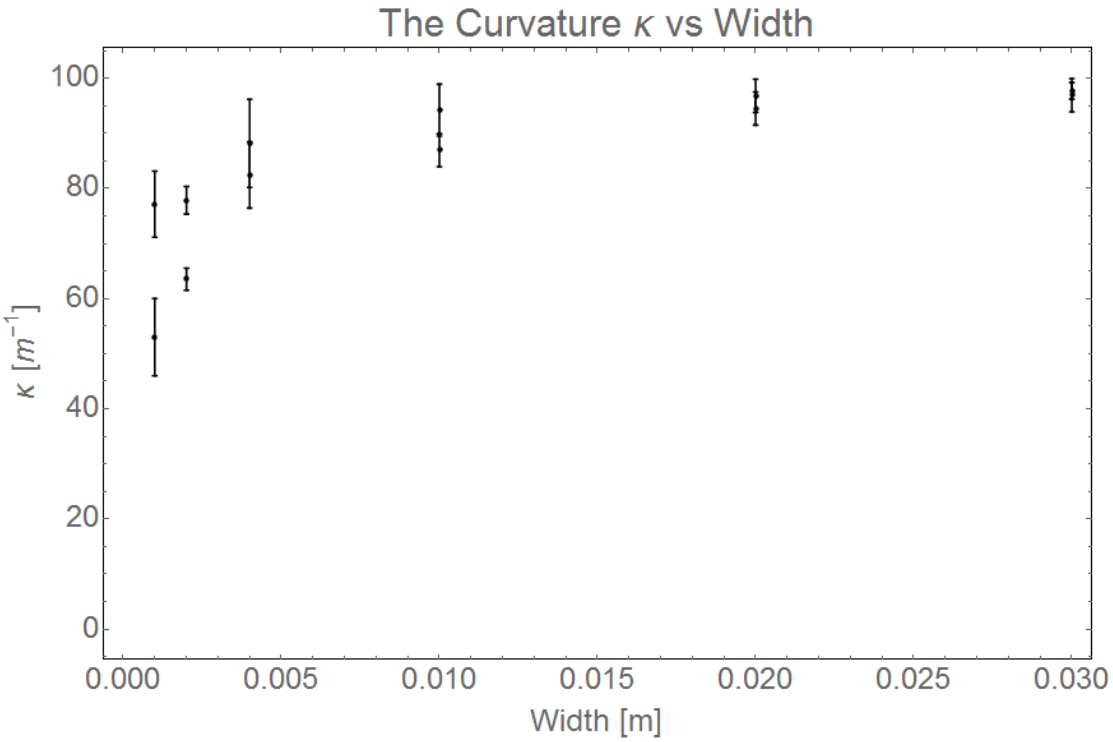

Figure 7 The curvature-width dependence for $\beta = 0.00017(3)$. The curvature of each strip was measured in two possible orientations separately.

It can be noted that for very narrow strips the asymmetry is significant. The boundary tension due to cutting is sufficiently large to have observable influence. But the wider the membrane is, the more negligible those effects are and the smaller the asymmetry. There is a visible trend showing that wider sheets bend more.
Unfortunately, it is impossible to predict what should the value be in the limit of width approaching the thickness (the membrane becoming a rod), since prediction made in [5] was done for not uniform spheroidal filaments. Thus it is largely overestimated. It can only be said that in that limit the curvature should be less than 175 m^{-1}.

The example picture of how the strip bends is shown on Figure 8.

Figure 8 The recovered side view shape of the membrane with dimensions 0.1 mm x 10 mm x 80 mm.

4.2 Rectangular sheets with aspect ratio of order of unity.

When the membranes become wide it was observed that they bend in two possible directions being the two lines of symmetry. The system is deterministic, but the random initial perturbation causes it to collapse into one or the other state. Intuitively, it is easier for a system to form a crest that is parallel to the width (in other words bend along shorter axis) because the bending moment (torque) is larger in this direction. But as the aspect ratio approaches 1, the preference of bending in one axis over the other vanishes.

An example of a bended membrane overlaid with a triangulation graph and a three dimensional shape recovered by the algorithm (section 3.2.1) is shown on Figure 9.

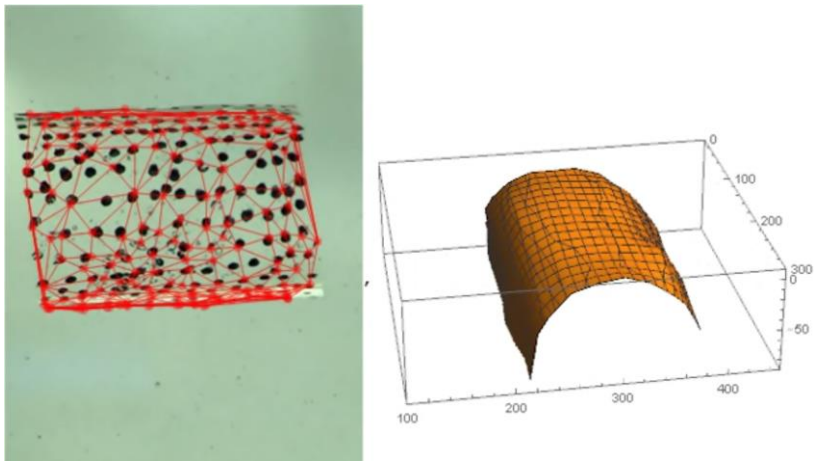

Figure 9 The bended along shorter axis membrane overlaid with a triangulation graph (red) and its three dimensional surface plot. The dimensions of the sheet are 0.1 mm x 40 mm x 56 mm

It was also observed that once the sheet has bent along one or the other axis, it had a tendency to incline. There are three possible explanations to this effect.
For one thing, it cannot be excluded, that inclination was produced solely because of viscous interactions with the walls or with the bottom of the container and if the container was large enough, then there would be no preferred inclination.
Secondly, it might be, that perfectly horizontal bended state is an unstable equilibrium and eventually all sheets will incline to a certain preferred settling angle.
There is a third possibility that the inclination arises by random initial perturbation so that one edge has bigger curvature than the other and the more bended side rises faster. When the curvature finally becomes uniform, the sheet would maintain its initial orientation as rigid bodies do [4]. It is certain however, that the timescale of this rotation is very large, so a very high and large container is necessary to verify either hypothesis.
An example of an inclined shape is shown on Figure 10.

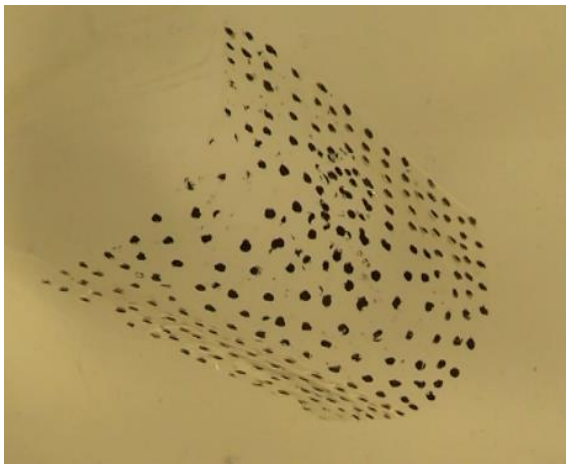

Figure 10 A picture of an inclined, bended along the shorter axis membrane. The dimensions of the membrane are 0.1 mm x 45 mm x 62 mm

4.3 Square sheets of thickness 0.05mm.

Sheets with thickness of 0.05 mm and length 55mm have $\beta = (9 \pm 1.5) \cdot 10^{-5}$. As they rise, the may collapse into one more possibly metastable state. The height of the beaker did not allow to verify, whether the system always eventually would escape it or whether it is a local equilibrium.
The photograph from above is shown in Figure 11:

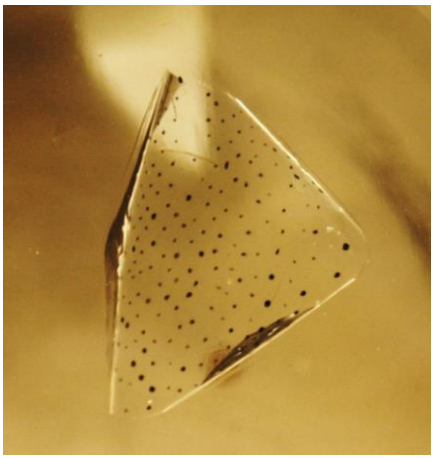

Figure 11 A third possibly metastable state. Two corners are buckled forming a sharp vertex (on the right hand side). The left hand side of the membrane has bent normally.

The configuration of this shape is triangle-like. One side of the membrane has bent normally, but the two corners on the other side have buckled separately in a competitive way. It is possible that this configuration is not stable as the projected area is large and it could be possible that the two corners will bend even more and finally reach the U-shaped equilibrium. However to verify this, a higher beaker is needed. If this configuration is indeed a metastable one, then it may be possible that all four corners might bend separately forming a square in the middle like an origami. This however was not observed in the experiments and if possible, it is hard to obtain.

4.4 Triangular sheet of thickness 0.05 mm.

An equilateral triangular sheet of thickness 0.05 mm and side 50 mm was recorded from top and the image (Figure 12) was obtained. The corners of the sheet have buckled, thus leaving a hexagonal-like projection.

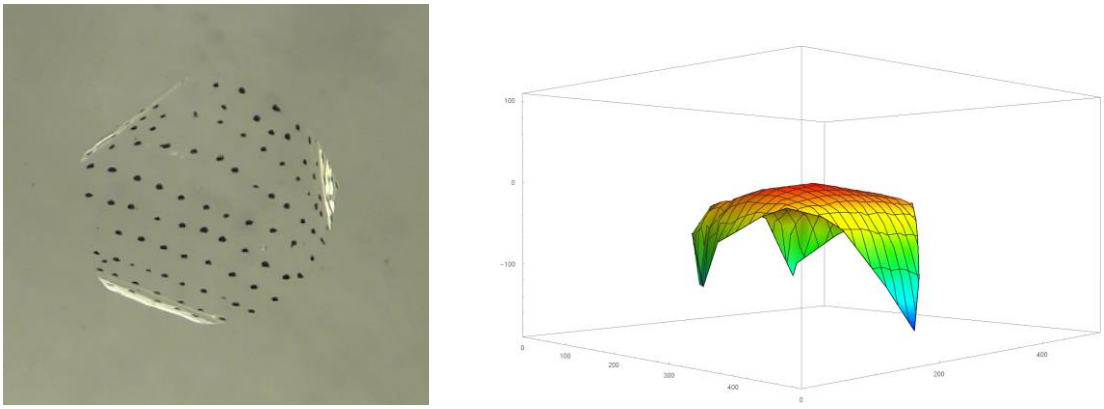

Figure 12 An equilateral triangular sheet of size 50 mm and thickness 0.05 mm as photographed from above (left) and its 3D shape as viewed from the side (right)

5. Areas of improvement

In further research a larger container should be used both in diameter and height to verify what causes bended sheets to incline and to gain assurance that the investigated shapes of the membranes are indeed stable. A numerical simulation should be written to investigate the stabilities of different states and the nature of the width dependence of the elasto-gravitational number. Quantitative investigation should be done with variety of shapes (e.g. circular, slender lattices, shapes with holes) at even thinner membranes. The trajectories and velocities of rising sheets should also be investigated.

6. Possible applications

Graphene is known to be one of the most stiff materials ever produced, having Young's Modulus of the order of terapascals [7]. But because it is also very thin, the bending stiffness is low. It is not straight-forward to tell what is the bending stiffness of a graphene monolayer since thin plate theory based on stretching and compression of outer and inner layers is not suitable for few layered graphene as it is not uniform [8]. Much work has been done to investigate the bending modulus of graphene both theoretically and experimentally and different approximations were proposed [7-9]. According to [8] the bending modulus of a monolayer graphene at room temperature is 7.1 eV, and of dilayer is 35 eV. Based on those values it can be calculated that the elasto-gravitational number of a graphene monolayer strip of length 5 micrometres merged in ethanol is 0.012, which is enough for a sheet to visibly bend. It is therefore possible that investigations on how thin sheets behave when sedimenting might be important in graphene printing.

7. Conclusions

The sedimentation/rising of thin membranes is a complex problem. The most important quantity called an elasto-gravitational number was introduced and shown that it is width-dependent and hence, the correction should be applied to account for it. The nature of the stable shapes was discussed. The method of obtaining the three dimensional shape was proposed and its limitations were discussed. The optical distortion of a cylindrical beaker was corrected and allowed to measure the curvature of thin strips accurately based on the photographs from the side. Finally, the possible future applications in graphene printing were discusses. There is still much work to be done both experimentally and theoretically in this field.

Appendix 1. The Mathematica implementation of the algorithm to recover 3D shape of the membrane.

```
    images = Flatten@Table[{
         napis = "Directory\\img" <> ToString[i] <>
".png";

         data = Quiet@Import[napis]
         }, {i, 2331, 0, -10}];
    pts = ImageFeatureTrack[images, MaxFeatures -> 400 ,
       MaxFeatureDisplacement -> 10];
    ppts = Transpose@pts;
```

```
    pt = Table[DeleteCases[ppts[[i]], _Missing], {i, 1,
Length[ppts]}];

    (*Deleting tracks which are incomplete*)
    l = Table[Length[pt[[i]]], {i, Length[pt]}] ;
    Length[l]
    del = DeleteCases[
       Table[If[l[[i]] < Length[images], {i}], {i,
Length[l]}], Null];

    p = Delete[Table[
        If[l[[i]] == Length[images],
         Table[pt[[i]][[j]], {j, 1, Length[pt[[i]]]}]
         ],
        {i, 1, Length[pt]}], del];
    ptrans = Transpose@p;
    ListLinePlot[p]

    Needs["ComputationalGeometry`"];
    dt = DelaunayTriangulation[ptrans[[1]]];
    toPairs[{m_, ns_List}] := Map[{m, #} &, ns];

    triang = Flatten@Table[{
         edges = Flatten[Map[toPairs, dt], 1];
         Graphics[
          GraphicsComplex[
           ptrans[[i]], {Line[edges], Red,
PointSize[Large],
            Point[ptrans[[i]]]}]]
         }, {i, 1, Length[images]}];

    e0 = Map[toPairs, dt];
    edges0 = Flatten[e0, 1];

    inc = Table[

       eidistmean = Table[
         Table[{ptrans[[k]][[i]][[1]],
ptrans[[k]][[i]][[2]],


EuclideanDistance[ptrans[[k]][[Last@dt[[i]]]][[j]],
            ptrans[[k]][[i]]]},
          {j, 1, Length[ptrans[[k]][[Last@dt[[i]]]]]}]

         , {i, 1, Length[dt]}]

       , {k, 1, Length[images]}];
    Length@edges0

    srodek = First@
      First@Position[ptrans[[1]],
        First@Nearest[ptrans[[1]], Mean[ptrans[[1]]]]]
    sr = ptrans[[1]][[srodek]]

    wami = Table[
       Table[Table[Infinity, {i, 1, Length@dt}], {j, 1,
Length@dt}], {t,
```

```
        1, Length@images}];
    le = Length@edges;
    li = Length@images;
    For[t = 1, t < li, t++,
     {
      wspsrodka = ptrans[[t]][[srodek]];
      For[e = 1, e <= Length@edges, e++,
       {


        i = edges[[e]][[1]],
        j = edges[[e]][[2]],

        wami[[t]][[i]][[j]] =

         Abs[Sqrt[
            ((Flatten[

inc[[1]][[i]][[Flatten@Position[Last@dt[[i]], j]]]][[
                3]])^2 - (Flatten[

inc[[t]][[i]][[Flatten@Position[Last@dt[[i]], j]]]][[
                3]])^2)]]*
           If[EuclideanDistance[{ptrans[[1]][[i]][[1]],
               ptrans[[1]][[i]][[2]]}, sr] >=
             EuclideanDistance[{ptrans[[1]][[j]][[1]],
               ptrans[[1]][[j]][[2]]}, sr], 1, -1]

        }]
      }]

    (*
    For cylindrical symmetry:
    If[EuclideanDistance[{ptrans[[1]][[i]][[1]],ptrans[[1
]][[i]][[2]]},\
    Mean[ptrans[[t]]]]>=EuclideanDistance[{ptrans[[1]][[j
]][[1]],ptrans[[\
    1]][[j]][[2]]},Mean[ptrans[[t]]]],-1,1]
    ,
    For axisymmetry:
    If[Abs[ptrans[[1]][[i]][[1]]-
ptrans[[1]][[srodek]][[1]]]>=Abs[ptrans[[\
    1]][[j]][[1]]-ptrans[[1]][[srodek]][[1]]],1,-1]

    *)

    wami2 = Table[Table[Infinity, {i, 1, Length@dt}], {j,
1, Length@dt}];
    For[e = 1, e <= Length@edges, e++,
     {

      i = edges[[e]][[1]],
      j = edges[[e]][[2]],

      wami2[[i]][[j]] =

Flatten[inc[[1]][[i]][[Flatten@Position[Last@dt[[i]],
j]]]][[3]]
```

```
      }]

    (*Constructing weighted graph, shortest path
function, and cetre of \
    the membrane*)
    g = WeightedAdjacencyGraph[wami2];
    short = FindShortestPath[g, All, All, Method ->
"BellmanFord"];

    ldt = Length@dt
    animacja = Table[
       heights = Flatten[Table[{
           trasai = short[srodek, k];
           ltr = Length@trasai;
           dl1 =
            Table[wami[[tt]][[trasai[[i]]]][[trasai[[i +
1]]]], {i, 1,
              ltr - 1}];
           ldl1 = Length@dl1;
           height1 = {ptrans[[tt]][[k]][[1]],
ptrans[[tt]][[k]][[2]],
             Sum[dl1[[j]], {j, 1, ldl1}]}
           }, {k, 1, ldt}], 1];
       imwidth = ImageMeasurements[images[[1]],
"Dimensions"][[2]];
       imheight = ImageMeasurements[images[[1]],
"Dimensions"][[1]];
       ListPlot3D[heights,
        PlotRange -> {{0, imwidth}, {0, imheight}, {-190,
110}},
        BoxRatios -> {imwidth, imheight, 300}, ImageSize
-> Large,
        ViewPoint -> {0, -2, 1},
        ColorFunction -> Function[{x, y, z}, Hue[.65 (1 -
z)]]]

       , {tt, 1, li - 1, 1}];


    film = MapThread[HighlightImage, {images, triang}];
    filmanim =
      Table[{Show[film[[i]], ImageSize -> Medium],
animacja[[i]]}, {i, 1,
        Length@animacja}];
    film[[1]]

Dynamic[Manipulate[filmanim[[tt]], {tt, 1,
Length@animacja, 1}]]
```

References

[1] G. K. BATCHELOR, Slender-body theory for particles of arbitrary cross-section in Stokes flow, J. Fluid Mech. 44 (1970), 419–440.

[2] R.G. COX, The motion of long slender bodies in a viscous fluid Part 1. General Theory, J. Fluid Mech. 44 (1970), 791–810.

[3] JASON E. BUTLER & ERIC S. G. SHAQFEH (2002). Dynamic simulations of the inhomogeneous sedimentation of rigid fibres. Journal of Fluid Mechanics, 468, pp 205-237 doi:10.1017/S0022112002001544

[4] HAPPEL, J. & BRENNER, H. 1965 Low Reynolds Number Hydrodynamics. Prentice Hall.

[5] L. LI, H. MANIKANTAN, D. SAINTILIAN, S. SPAGNOLIE, The sedimentation of flexible filaments, J. Fluid Mech., 735, 706-736 (2013)

[6] Glycerine Producers' Association. *Physical properties of glycerine and its solutions.* New York: Glycerine Producers' Association; 1963.

[7] LEE, C., WEI, X., KYSAR, J. W. & HONE, J. Measurement of the Elastic Properties and Intrinsic Strength of Monolayer Graphene. Science321, 385-388, doi:10.1126/science.1157996 (2008).

[8] N. LINDAHL, D. MIDTVEDT, J. SVENSSON, O. NERUSHEV, N. LINDVALL, A. ISACSSON, E.E.B. CAMPBELL. Determination of the bending rigidity of graphene via electrostatic actuation of buckled membranes. Nano Lett. 12, 3526–3531 (2012).

[9] Q. LU, M. ARROYO, R. HUANG, Elastic Bending Modulus of Monolayer Graphene, J. Phys. D: Appl. Phys.42 (2009).